Russian Journal of Earth Sciences

Optimal Interpolation Method for Generating a Digital Bathymetric Model for Shallow Waters: A Case Study over Mauritius Coast

S. Satpute[1], S. Roy[2], O. S. Gatage[3], V. B. Kolase[3], S. K. Singh[1], and G. Dandabathula[*,2]

[1]Centre for Climate Change and Water Research, Suresh Gyan Vihar University, Jaipur, India
[2]Regional Remote Sensing Centre – West, NRSC/ISRO, Jodhpur, India
[3]Department of Geography, Bharathidasan University, Tiruchirappalli, India
* **Correspondence to:** Giribabu Dandabathula, dgb.isro@gmail.com

Abstract: Bathymetry unveils the underwater topography of oceans, seas, rivers, and lakes. It is a fundamental data resource for various applications, like physical oceanography, marine geology, geophysics, and marine resources. The techniques to compute the seafloor depths are ship-borne echo sensors, empirical models of satellite-derived bathymetry, and aerial-space-borne laser altimetry. The digital bathymetric surfaces are generally generated from a distributed seafloor depths. Once these depth points are collected, the next step to generate a continuous surface is to select and implement interpolation. Numerous interpolation methods have advantages and disadvantages that can hamper the accuracy of the surface, which generally depends on the shape of the extent, distribution, and point density. To date, there is no recommended interpolation method when the study extent is circular with well-distributed points – the core objective of this research is oriented towards this. An attempt was made to generate a digital bathymetric surface for the Mauritius coast with ~ 1.2 million depth points accrued from the NASA ICESat-2 geolocated photons and sounding depths from the marine charts. These points were used as input to interpolation methods like Inverse Distance Weighted, Natural Neighbour, and various forms of Ordinary Kriging. Our findings show that all the methods have generated visually similar surfaces, but the Inverse Distance Weighted interpolation has given the output with less quantified uncertainty.

Keywords: Bathymetry, Interpolation, LiDAR, Inverse Distance Weighted, Natural Neighbour, Kriging.

Citation: Satpute, S., S. Roy, O. S. Gatage, V. B. Kolase, S. K. Singh, and G. Dandabathula (2024), Optimal Interpolation Method for Generating a Digital Bathymetric Model for Shallow Waters: A Case Study over Mauritius Coast, *Russian Journal of Earth Sciences*, 24, ES6003, EDN: PGHFFW, https://doi.org/10.2205/2024es000937

Research Article

Received: 4 July 2024
Accepted: 30 September 2024
Published: 30 December 2024

Introduction

Bathymetry is the study of mapping the water depth in oceans, seas, rivers, and lakes, and it plays an essential role in understanding and portraying the marine environment. Similar to topographic mapping on land, bathymetric surveys create seafloor depth maps, revealing its seabed structure [*Vogt and Tucholke*, 1986]. This information is essential for various applications, including marine navigation, ocean engineering, seafloor morphology, tectonic studies, and deep-sea mineral exploration [*Dysart*, 1996; *Smith and Sandwell*, 1997; *Vogt and Tucholke*, 1986; *Wölfl et al.*, 2019]. Bathymetric data potentially aids in investigating coastal dynamics, sediment transportation, changes in seabed morphology, sea level changes, and the impact of global climate patterns, and also helps avoid underwater hazards during navigation [*Smith and Sandwell*, 1997; *Wölfl et al.*, 2019].

Technological advancements have dramatically improved our ability to map the ocean floor. Ship-borne echo-sounding techniques are classical but still are valid methods for collecting bathymetric data [*Smith and Sandwell*, 1997]. The echo-sounding techniques are generally either single-beam or multi-beam; if single-beam echo sensors are employed, the

result is less coverage, whereas the multi-beam echo-sounding sensors can provide better coverage and more detailed underwater topography [*Ashphaq et al.*, 2021; *Pratomo et al.*, 2023].

With the advent of the earth-observation systems, satellite-derived bathymetry methods that came into existence use multispectral imagery to map the depths of the shallow waters. However, for these methods are empirical and need real-time seed data as a parameter to initiate the model [*Wölfl et al.*, 2019].

On the other hand, LiDAR-based bathymetry has several advantages over ship-borne sounding technology. These advantages include high precision, high point cloud density, high accuracy, and low cost [*Ashphaq et al.*, 2021; *Hilldale and Raff*, 2007; *Li et al.*, 2023]. However, the limitation with the LiDAR-based altimeter is that we can measure to limited depths [*Ashphaq et al.*, 2021; *Li et al.*, 2023]. Ice, Cloud and land Elevation Satellite-2 (ICESat-2), launched by the National Aeronautics and Space Administration (NASA), has been operational since September 2018. ICESat-2 hosts a solo sensor, Advanced Topographic Laser Altimeter System (ATLAS), credited as a revolutionary space-borne altimeter due to its caliber with a highly sensitive photon-counting system [*Markus et al.*, 2017]. The ATLAS sensor onboard the ICESat-2 utilizes a 532 nm wavelength (green) laser, operating at a pulse repetition frequency of 10 kHz, and encounters a diffractive optical element to release six beams. From each of the six beams, geolocated photon data having a spatial resolution of 70 cm can provide surface elevation information [*Neumann et al.*, 2019]. Primarily, the applications of the ICESat-2 data were oriented for the cryosphere. However, the scientific fraternity has successfully used geolocated photon data for various applications related to land/terrain, forest/canopy, and inland water bodies [*Brown et al.*, 2023].

Parrish et al. [2019] evaluated the application validity of ICESat-2-based geolocated photon data towards bathymetric studies; their studies proved that seafloor detection in water depths of up to ~ 40 m is possible during clear water conditions [*Parrish et al.*, 2019]. With this clue, numerous studies have shown the potential of using ICESat-2 geolocated photons for bathymetric studies [*Giribabu et al.*, 2023, 2024; *Guo et al.*, 2022; *Ranndal et al.*, 2021; *Xie et al.*, 2021].

In our study, we generated a digital bathymetric model for the shallow waters of the coastal area for an island using the depth information from ICESat-2 geolocated photon data and the sounding depth values from the available hydrographic charts. The points representing the depth values need interpolation to generate a surface representing the seafloor topography. Interpolation is a mathematical process to predict unknown values using the surrounding measured values [*Burrough et al.*, 2015]. Interpolation techniques are generally classified into deterministic and geostatistical [*Childs*, 2004]. Deterministic interpolation techniques create surfaces based on measured points (with known values) using mathematical formulas; methods such as Inverse Distance Weight (IDW) and Natural Neighbor (NN) fall in the deterministic category. In contrast, geostatistical interpolation techniques, such as various forms of Kriging, are based on statistics and are used for predicting surface values but include some measure of the uncertainty [*Childs*, 2004].

However, many researchers are still investigating the best choice in selecting the optimal interpolation technique while generating a bathymetric surface for the shallow water regions, and the question remains a gap area [*Li et al.*, 2023]. The motivation of this study is to determine the best optimal interpolation method given a set of points representing depth values in a shallow water region. Moreover, our research has emphasized an Island that is typically circular. Globally, many of the Islands are circular; thus, the anticipated results from this study should provide a clue for selecting the best interpolation method while generating a bathymetric surface.

Towards reaching the objectives of this research, after accruing the points data containing the depth values of the seafloor pertaining to the study area, various interpolation methods were used to generate the surfaces. Currently, in Geographic Information System (GIS) software like ESRI ArcGIS AND QGIS, nearly 40 interpolation methods are available.

Certain interpolation methods are optimized for surface generation, some for weather forecasting, and some for estimating the missing values. Research done by *Henrico* [2021] suggested that interpolation methods like IDW, NN, and various Ordinary Kriging (OK) forms are optimized for surface generation. These methods were given preference in our research to generate surfaces. These surfaces were validated by referring to the check-points and computing an error quantifier based on a statistical formula like Root Mean Square Error (RMSE). The RMSE computed for each surface generated form the individual interpolation method has been compared to assess the best interpolation method.

Material and methods

Study Area. The study area chosen for this research is Mauritius, which extends over 2.3 million km^2 (including its sea-zone). It is an island country in the Indian Ocean, about 2000 km off the south-eastern coast of East Africa and east of Madagascar. Isles like Rodrigues, Agaléga, and St. Brandon (Cargados Carajos shoals) are also part of Mauritius. The mainland Mauritius is at latitude 20°10 'S and longitude 57°30 'E, has a surface area of 1859 km^2 and a nearly 200 km long coastline. The region is mainly composed of different shoreline types, and chiefly, they are categorized as sandy, rocky, muddy, mixed, calcareous lime stones, and cliffs of coastal geological features [*Doorga et al.*, 2021]. Figure 1 shows the extent of Mauritius as viewed in high-resolution satellite imagery. The Island is of volcanic origin, and its formation involves the three primary dome building processes that created the structural shape of the high uplands in the central region and lowlands in the coastal region [*Doorga et al.*, 2021]. According to recent estimates, Mauritius Island has a population of 1.27 million, with the main attraction being its coastal beaches for tourists. Tourism is the third pillar of economic growth after Mauritius's manufacturing and agriculture sectors [*Duvat et al.*, 2020]. Mauritius's central Plateau is between 300 to 600 meters from mean sea level.

In the context of global climate change, Mauritius is highly vulnerable to sea-level rise as recent studies indicate a rise of 5.6 mm/year on average over the past 30 years – this is 2 to 3 times faster than the 20th century global mean sea level due to climate change [*Devi and Xi*, 2020]. This, in turn, will impact the increase in coastal erosion [*Becker et al.*, 2019]. Thus, high-resolution digital bathymetric data, like the one generated in this research, is beneficial for studying climate change's impact on Mauritius's coastal line. In this research, we have generated a digital bathymetric model for a buffer region of 3 km from the coastline of Mauritius mainland (shown in Figure 1b)

Datasets. Table 1 shows the datasets used to generate a digital bathymetric model for Mauritius Island. Primarily, the datasets include NASA ICESat-2 geolocated photons, navigational charts, and elevation values from a bare-earth digital elevation model (DEM). The details of these datasets are mentioned in the subsequent sections.

ICESat-2, a polar-orbiting satellite from an average altitude of 496 km, will acquire the data during day and night for the globe in 1387 predefined ground reference tracks with a temporal resolution of 91 days [*Markus et al.*, 2017]. Over the extent of Mauritius mainland and its shallow waters coasts, eight ICESat-2 reference ground tracks are available (listed in Table 1 and illustrated in Figure 2). From these eight reference ground tracks, one hundred sixty acquisitions of ICESat-2 data between October 2018 and October 2023 are available for the study area. In general, bathymetric studies should use only those acquisitions from nighttime because daytime acquisitions can include substantial noise arising from solar background radiations [*Giribabu et al.*, 2023]. Similarly, ICESat-2 acquisitions may be impacted due to the presence of clouds, and photons may not be able to reach the Earth's surface [*Hawker and Neal*, 2021]. Thus, 79 acquisitions were available for retrieving the seafloor depth information by omitting daytime acquisitions and those of missed data due to the presence of clouds.

The sciences teams of ICESat-2 will process and distribute the photon data by categorizing it into various levels, out of which Level-2A data product, namely, ATL03, is

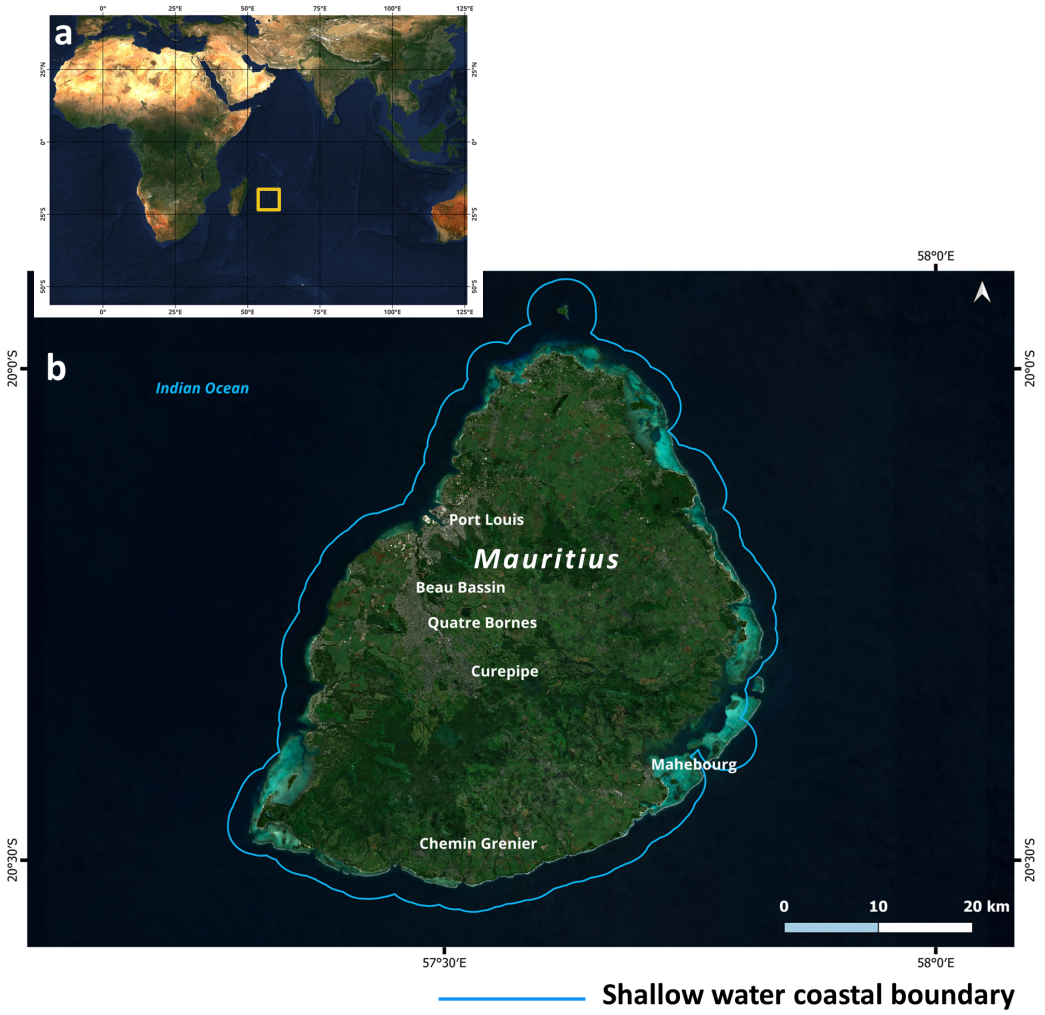

Figure 1. Location map of Mauritius mainland. (a) The location of the Mauritius mainland in the Indian Ocean is highlighted with a yellow box. (b) Mauritius mainland, which constitutes the study area of this research.

a principal data source that contains geolocated photons with attributes like latitude, longitude, and elevation for each successful photon event [*Neumann et al.*, 2019]. In our research, we have used ATL03. From the available 79 acquisitions over the study area, 474 beams are qualified for seafloor depth retrieval (shown in Figure 2). Retrieval of the seafloor from these beams is discussed in the methodology section.

The other source of seafloor depth is the navigational chart obtained from the National Hydrographic Office of the study area [*INHO*, 2024]. The sounding depths from chart number 2557 at a scale of 1:125,000 were manually digitized in GIS software. Elevation values for the mainland of the study area were retrieved from a bare-earth digital elevation model called Forest and Building removed Copernicus DEM (FABDEM); however, the role of the elevation values from the FABDEM is to fill the gap due to the Mauritius mainland during the visualization of the output and does not have any role in the generation of bathymetric model [*Hawker and Neal*, 2021].

Methodology. In general, during the ICESat-2's data acquisition process, photons emanating from the ATLAS sensor will return from various features of the Earth's surface. 2D profiles drawn from the along-track geolocated photons will enable us to visualize various features of the Earth's surface. As shown in Figure 3, for a subset of geolocated photons

Table 1. Details of the datasets used in generating a digital bathymetric model for the shallow waters of Mauritius coasts

Dataset	Source	Details
NASA ICESat-2 ATL03	OpenAltimetry application available at [*National Snow and Ice Data Center*, 2023]	Ground Track: 1217, 661, 272, 1103, 714, 158, 1156, and 600. Duration of Acquisitions: October 2018 to October 2023 Preferred acquisition period: mostly Night time Preferred beam type: Mostly strong beam Total number of Refracted photons from the seafloor: 1.2 million
Sounding depths from navigational charts	Information available at National Hydrographic Office's web portal available at [*INHO*, 2024]	Chart Name: Mauritius Chart Scale: 125000 Year of Publication: 2019 Chart No.: 2557
Forest and Building removed Copernicus DEM (FABDEM)	Web portal available at [*Hawker and Neal*, 2021]	Elevation values pertaining to the Mauritius mainland

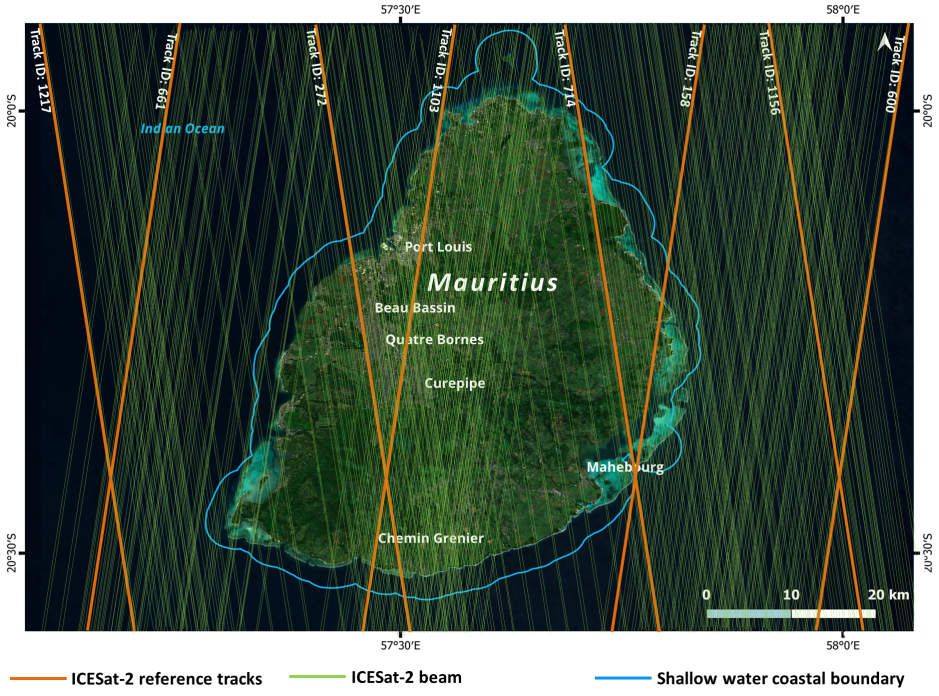

Figure 2. ICESat-2's ground reference tracks and available beams over Mauritius mainland and the surrounding shallow waters.

acquired over the region, namely, Centre de Flacq, which is adjacent to the coastal area, the profile shows the photons returning from the canopy, land, water surface, water column, and seafloor. In this research, all the ATL03 beams from the ICESat-2 were processed in ESRI ArcGIS software [*ESRI*, 2024a]; specifically, the graph wizard in the table editor of the ESRI ArcGIS facilitates provision for classification of the points falling in various classes (refer to Figure 3c). As this research is oriented to generate a bathymetric surface, the

photons returning from the canopy, land, and the water surface have been discarded – only those photons returning form the seafloor are considered for further steps.

Parrish et al. [2019], *Guo et al.* [2022], and *Giribabu et al.* [2024] suggested that before considering the depth information from the geolocated photons to generate the bathymetric surface, a refraction correction is a must; this is because there will be a change in the speed of light that occurs at the air-water interface due to different refractive indices of air and sea-water. Hence, the default depth information from the geolocated photons is apparent. This apparent depth can be corrected using Snell's Law as suggested by [*Giribabu et al.*, 2024; *Guo et al.*, 2022; *Parrish et al.*, 2019]. Similarly, the default vertical datum of the elevation/depth retrieved from the ATL03 data product is in the WGS84 ellipsoid system, whereas the seafloor depth in the bathymetric charts is represented in the orthometric system. In this research, the conversion of the depth information from the ellipsoidal to the orthometric system was done using the geoid height calculator available at the UNAVCO web portal by preferring the EGM2008 geoid model [*GAGE Facility*, 2021]. A total of 1.2 million depth values from the geolocated photons were accrued in this research for the shallow waters surrounding Mauritius.

Additionally, sounding depths were digitized from the navigational charts available at the National Hydrographic Office (NHO). A total of 22700 sounding depths were accrued for the shallow waters surrounding the coast of Mauritius.

Twenty-five depth points from the ICESat-2 geolocated photons were reserved as checkpoints to evaluate the output's accuracy (discussed in the subsequent sections). All the points representing the depths in the study area are illustrated in Figure 4. The methodology adopted for generating the surface from these points was incorporated in Figure 5.

An interpolation method is used to generate a continuous surface from the depth points, during which it will estimate a value in the area of unknown values from a distribution of known depth points to generate a continuous surface. In our research, we used the interpolation methods available in ESRI ArcGIS software [*ESRI*, 2024a]; the methods are shown in Figure 5.

The IDW is considered a non-statistical interpolation method and does not account for the spatial distribution of points but instead predicts unknown values based on the proximity of known values [*Li and Heap*, 2014; *Wang et al.*, 2014]. By giving preference to the nearest neighboring points, IDW assigns more influence to data points closer to the unknown points. These nearby known points carry greater weight in the calculation, and the unknown values are estimated as a weighted average of these close neighbors. It is proven that IDW will generate a smooth interpolated surface and considers dimension parameters, the number of sampling points, and the power parameter, which controls the influence of neighboring points on the interpolated values [*de Souza et al.*, 2003]. However, favoring the closest neighboring points results in weighted averages similar for all points in proximity, which can be a disadvantage using this method.

Similar to the IDW, NN interpolation method estimates unknown values using nearby known data points, but the difference is in computation approach. NN interpolation finds the closest subset of input samples to a query point and applies weights to them based on proportionate areas to interpolate a value; the method is also referred as Sibson or area-stealing interpolation [*Sibson*, 1981]. NN interpolation methods is having advantage that it works equally well with irregularly distributed points and also, will not produce errors like sudden peaks or sinks [*Watson*, 1992].

Kriging a geostatistical interpolation method uses the spatial correlation between sampled points to interpolate the values in the spatial field: the interpolation is based on the spatial arrangement of the empirical observations rather than on a presumed spatial distribution model. Kriging also generates estimates of the uncertainty surrounding each interpolated value [*Collet et al.*, 2018; *Luo et al.*, 2007]. Generally, during the process of estimating the optimal interpolation weights, Kriging method takes into account both distances and directions to establish the spatial relationships within the data. Ordinary Kriging is the most common form of interpolation method that uses to model the empirical semi variogram like spherical, circular, exponential, Gaussian, and linear.

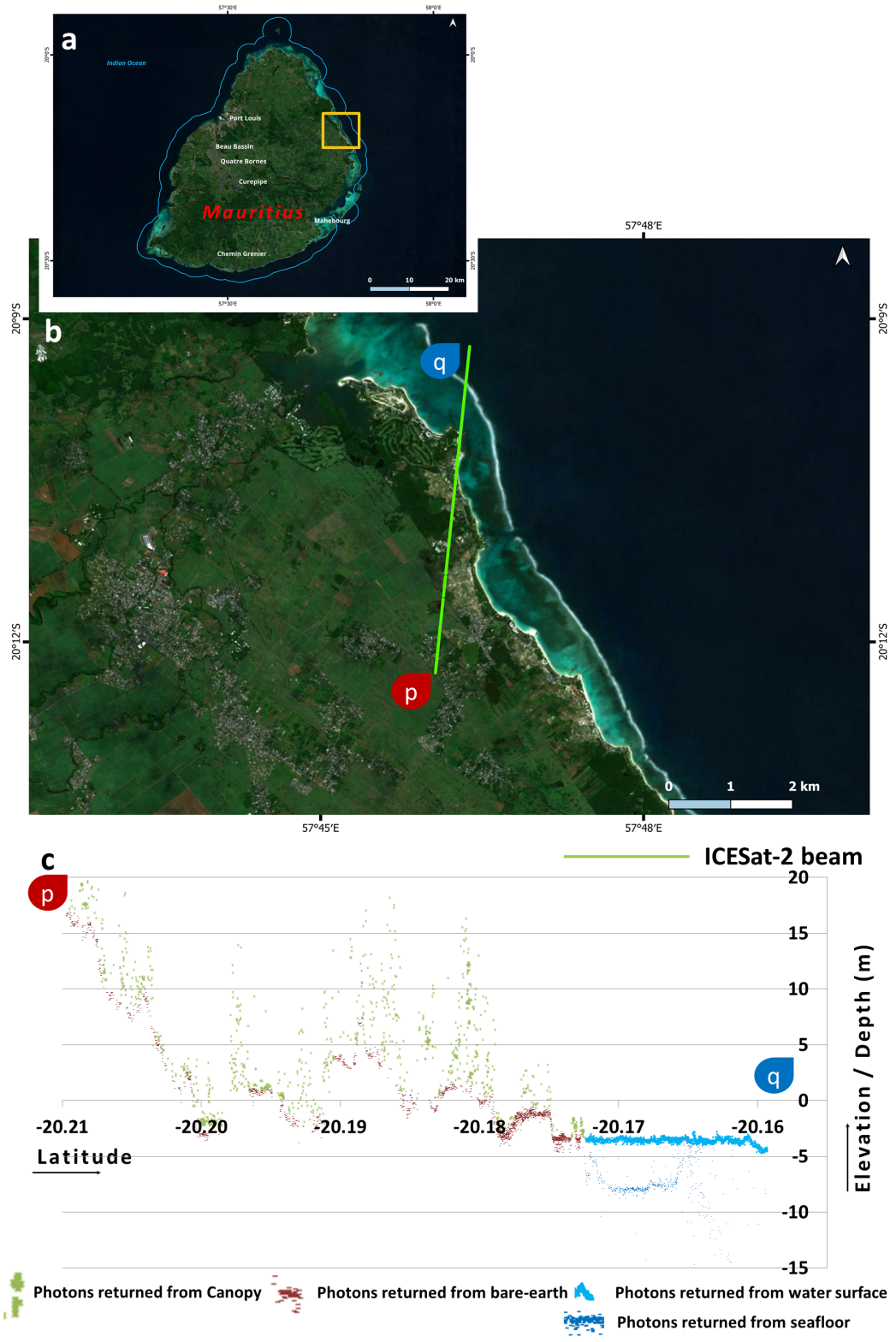

Figure 3. Return photons of ICESat-2 from various features of Earth's surface. (b) Location map of Mauritius mainland. (a) A subset of ICESat-2 beam acquired over land and shallow waters. (c) 2D profiles generated from along-track ICESat-2 geolocated photons. Notably, the profiles show the photons returned from canopy, land, water surface, water column, and seafloor.

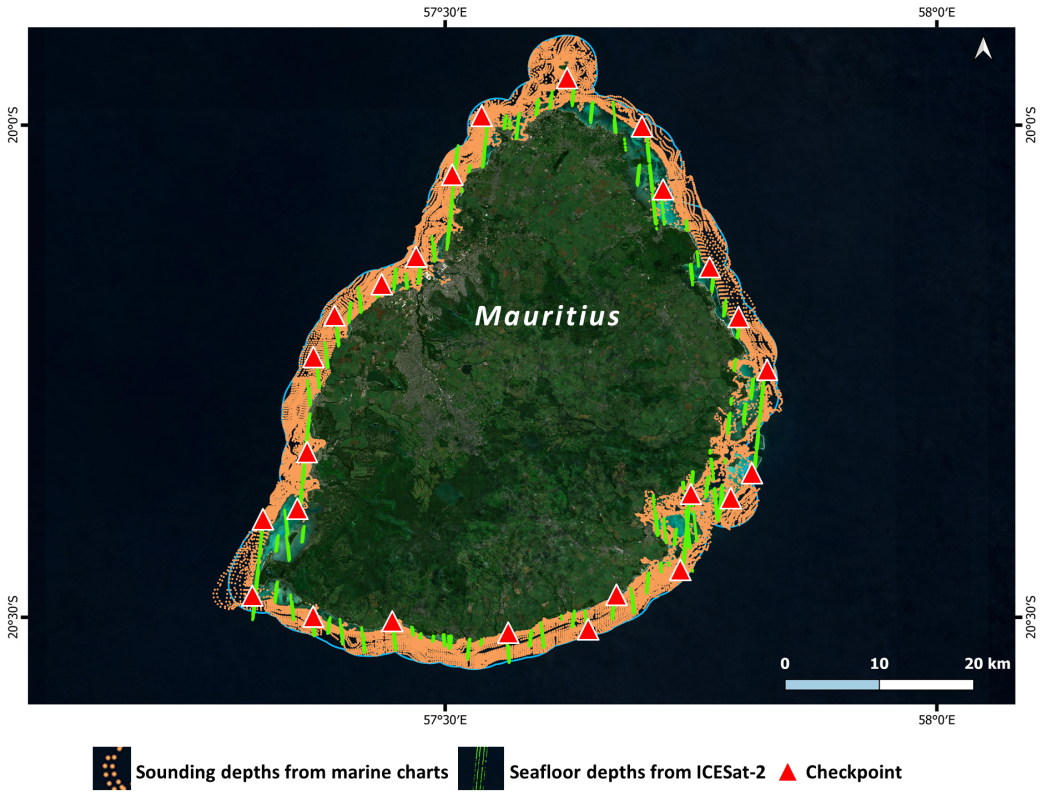

Figure 4. Map showing the distribution of points representing the seafloor depths used to generate a digital bathymetric model for the shallow waters of the Mauritius coast. Nearly 1.2 million points were accrued towards creating the depth database primarily acquired from the ICESat-2 geolocated photons returned from the seafloor and 22,700 sounding depths from marine charts. A few points were reserved as checkpoints for technical validation of the output.

Spatial autocorrelation in the spherical Kriging model increases linearly for short distances and then flattens after a certain threshold. This method is commonly used due to its moderate complexity and effectiveness for many spatial data types. Kriging interpolation with circular semi-variograms assumes that spatial correlation decreases in a circular pattern. This makes it suitable for data with a limited spatial extent and a rapid decline in correlation with distance. The spherical and circular Krigings methods work well when the area of study is relatively small, and the influence of known points diminishes quickly (very short distance) as you move away from them [*ESRI*, 2024b; *Mesić Kiš*, 2016].

Exponential Kriging assumes that spatial correlation decreases exponentially with distance. This method is ideal for data where the correlation declines rapidly over short distances, reflecting a more abrupt change in values as you move away from known points [*Mesić Kiš*, 2016]. The Gaussian Kriging model's spatial correlation decreases rapidly near the origin and more slowly over longer distances. This approach is well-suited for data with strong short-range correlation and a gradual decline over longer distances, providing a smooth transition in the interpolated values [*ESRI*, 2024b]. Linear Kriging assumes a steady, linear decrease in spatial correlation without a clear range limit. This method is appropriate for data where the correlation consistently declines over distance, without a point where the influence of known points becomes negligible.

Each Kriging method can be chosen for its suitability to different spatial patterns and data characteristics, ensuring accurate and reliable interpolations. By using the strengths of various kriging techniques, the research aims to understand the spatial relationships within the study area thoroughly.

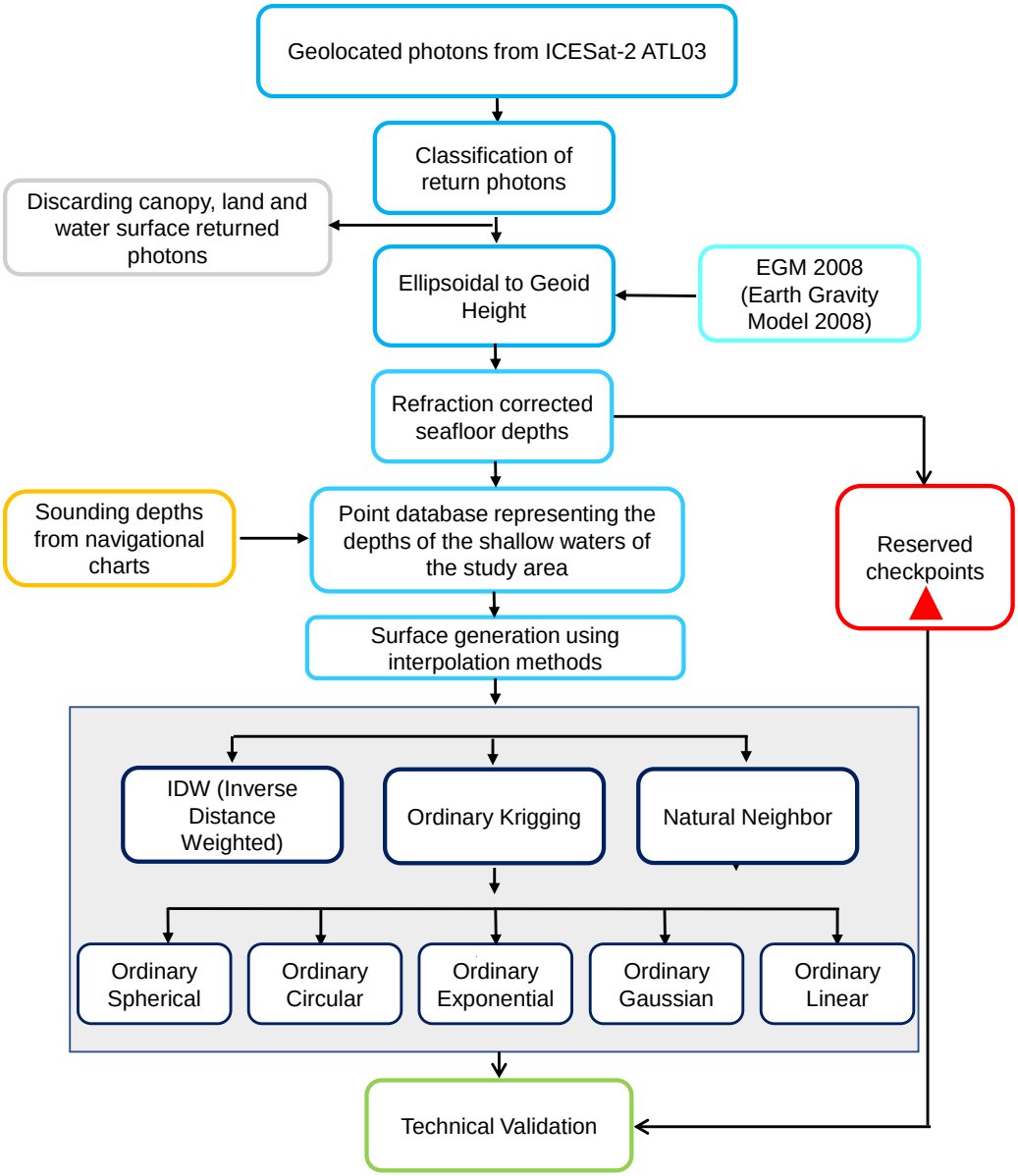

Figure 5. Schematic representation of the methodology used to generate a bathymetric surface from ICESat-2 geolocated photons and sounding depths from the marine charts. Bathymetric surfaces have been generated using various interpolation methods. The reserved checkpoints were not used in the interpolation methods and used for technical validation as reference points.

After generating the digital bathymetric surface using various interpolation methods, a technical validation was performed to assess the accuracy of each interpolation method. Twenty-five checkpoints that were well-distributed in the study area were used to validate the individual surface; during this process, the RMSE was calculated by comparing the depth values of each surface to that of the checkpoint. RMSE, provides a quantitative measure of the differences between the interpolated values and the observed values. This comparison allows evaluating the performance of each interpolation method. The formula for the RMSE is given in (1).

$$\Delta H = (\text{Depth})_{\text{bathymetric\_surface}} - (\text{Depth})_{\text{checkpoint}},$$

$$\text{RMSE} = \sqrt{\frac{\sum \Delta H^2}{n}}, \tag{1}$$

where $(\text{Depth})_{\text{bathymetric\_surface}}$ is the set of depth values obtained from the interpolated surface and $(\text{Depth})_{\text{checkpoint}}$ are the set of depth values of the reserved checkpoints of ICESat-2, $n = 25$ is the number of observations.

Results

Seven surfaces representing the digital bathymetric models were generated for the study area using IDW, NN, and five methods of Kriging interpolations. Figures 6 and 7 show the 3D perspective view and 2D maps of the digital bathymetric models generated from the IDW and other interpolation methods, respectively. Table 2 shows the RMSEs obtained for each surface, referring to the depth values of the checkpoints.

Errors in digital surfaces are usually classified as either sinks or peaks/spikes. A sink is an area surrounded by higher elevation values and referred to as a depression or pit. Generally, sinks appearing suddenly on the surfaces are treated as imperfections in the digital surfaces. Likewise, a peak/spike is an area surrounded by cells of lower value. The more sinks and peaks/spikes appear in the modelled surfaces implies severe errors. Errors such as these can be visualized by performing quality assessment through visual analysis.

For our research towards the technical validation of the outputs, in the first stage, qualitative analysis was done using the visual analysis of the surfaces obtained from all the interpolation methods; the result from the qualitative analysis shows that all the digital surfaces are without any sinks and spikes (refer to Figures 6 and 7). Earlier, Amoroso et al. investigated the influence of point density on the accuracy of bathymetric surface generation and concluded that more dense and well-distributed points could ensure better surface generation [*Amoroso et al.*, 2023]; probably, this may be the reason that in our case, the surfaces generated by various interpolation methods have yielded less visible errors. However, quantifiers like RMSE can inform the invisible uncertainty in the digital surface. The resultant RMSEs, as computed based on (1), were as summarised in Table 2 for quantifying the depth accuracy of individual surfaces. From Table 2, the IDW interpolation method has yielded significantly lower RMSEs when compared with the other interpolation methods. The minimum and maximum differences in the depth estimations in the surface generated by IDW are 0.28 m and 0.96 m, respectively. Next to the IDW interpolation, NN is a better estimation of depths (refer to Table 2). Notably, the RMSEs obtained from the surfaces of various forms of Kriging methods have yielded nearly 1 m or greater of error. Thus, the depth estimation given by the IDW, which has a minimum uncertainty of ~ 0.68 m, stands to be a better performer.

Table 2. RMSEs obtained for bathymetric surface that were generated from various interpolations methods

Interpolation method	RMSE (m) $n = 25$	Minimum (ΔH)	Maximum (ΔH)
IDW	0.68	0.28	0.96
NN	0.89	0.45	1.04
OK – Spherical	0.98	0.68	1.33
OK – Circular	1.23	0.82	1.32
OK – Exponential	1.45	0.83	1.34
OK – Gaussian	1.46	0.72	1.65
OK – Linear	1.12	0.69	1.55

Discussion

This study aimed to evaluate the accuracy of three interpolation methods – IDW, NN, and various parametric methods of Kriging in predicting the bathymetry of the shallow waters of the Mauritius coastal region. The research ensured a comprehensive distribution of sample points across the entire study area by utilizing depth points retrieved from the

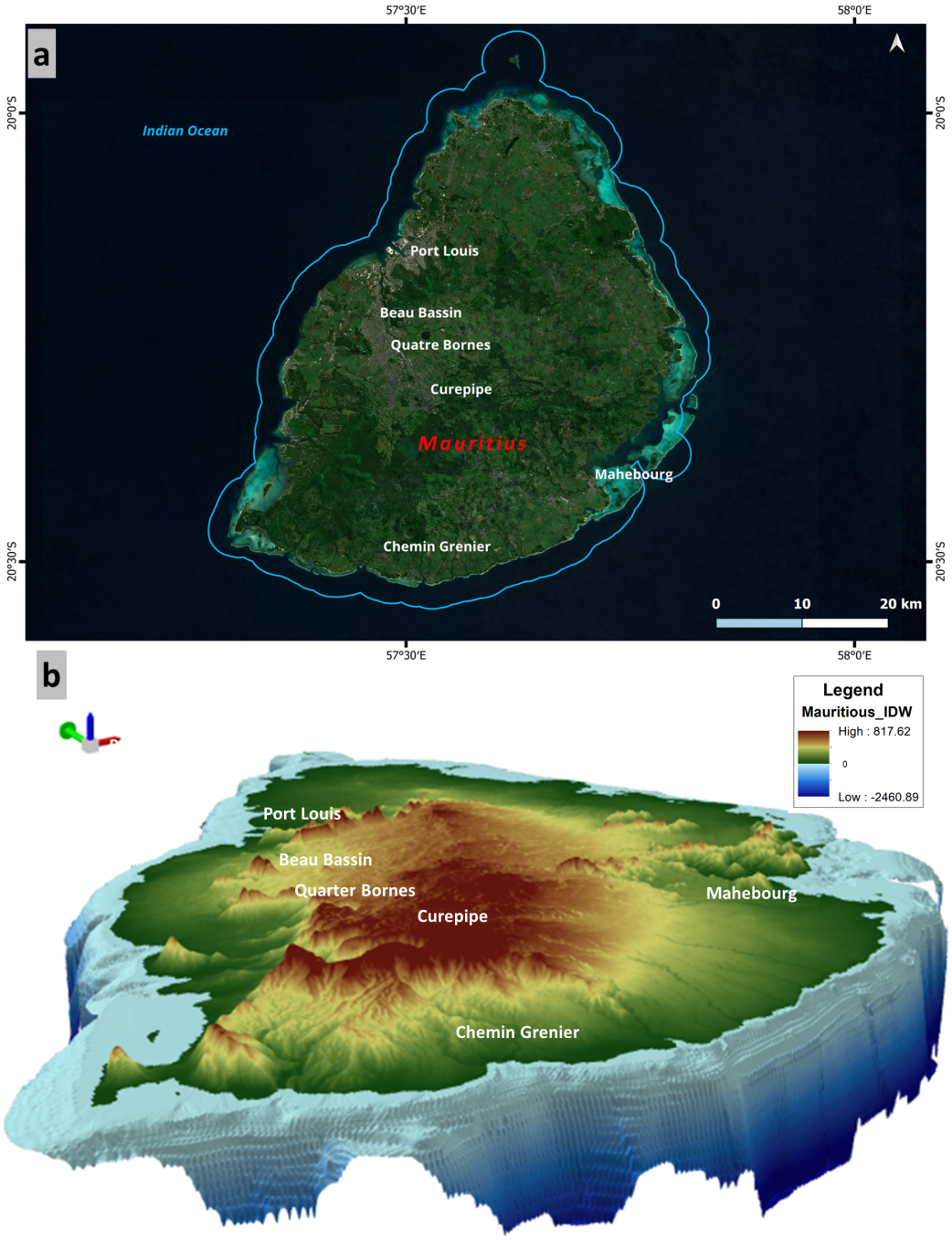

Figure 6. 3D perspective generated with a 10 m digital bathymetric model generated using ICESat-2 photons and sounding depths from the navigation charts for the extent of Mauritius. (a) Extent showing Mauritius mainland and the surrounding coast in a high-resolution satellite imagery. (b) Perspective view for the extent of Mauritius and its surroundings.

water-penetrated geolocated photon data of ICESat-2 and the accurate sounding points digitized from the navigation charts.

Earlier, Ferreira et al. conducted a similar experiment at the main damming of the Sao Bartolomeu stream located at the Federal University of Viçosa in Brazil. In their experiment, the distribution of the points is linearly spread but interleaved, and the extent of the study area is nearly rectangular. Their experiment proved that the OK method produced superior

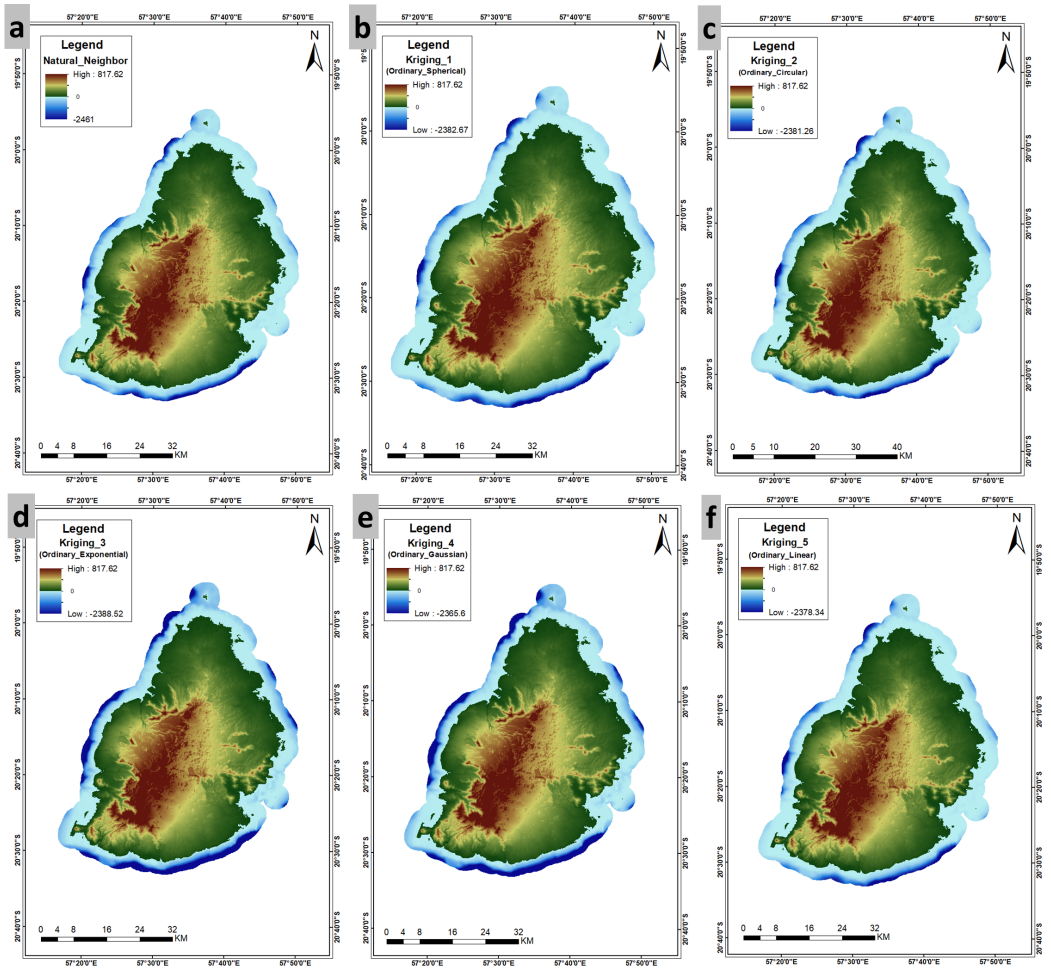

Figure 7. 2D maps of the digital bathymetric model generated using ICESat-2 photons and sounding depths from the navigation charts for the extent of Mauritius. (a, b, c, d, e, & f) Bathymetric models generated from NN, OK (spherical, circular, exponential, Gaussian, and linear), respectively.

output to IDW [*Ferreira et al.*, 2017]. Whereas, the experiment conducted by Henrico et al. [*Henrico*, 2021] over the extent of Saldanha Bay, which is nearly irregular in shape and having well-distributed points, has proven that IDW has given superior quality of surface prediction in comparison with the OK method.

The shape of the study extent in our research is nearly circular with a well-distributed depth points. The surfaces generated from various interpolation methods when performed visual comparisons, revealed clear similarities in how these methods estimate and generated continues bathymetric surface. However, quantitative assessment resulted in informing that the IDW method has unleashed a surface with fewer uncertainties. Consequently, IDW was identified as the most suitable interpolation method for predicting the bathymetry of the Mauritius coast. Compared to NN and OK methods, IDW produced better accuracy predictions. The findings illustrate the effectiveness of IDW in bathymetric mapping and highlight its potential as the preferred method for future studies in similar coastal environments.

Conclusion

This study aimed to identify the optimal interpolation method for generating a high-resolution digital bathymetric model for a circular-shaped extent with well-distributed points. Towards this, the coastal area of Mauritius Island containing shallow waters was chosen as a study area. Approximately 1.2 million depth points from ICESat-2 photons and

navigation charts were used as input to the interpolation methods. IDW, NN, and various Kriging interpolation methods were used to generate bathymetric surfaces. Technical validation was performed through qualitative and quantitative assessments. Visual analytics shows similarities in all the output surfaces. In contrast, the quantitative assessment has shown that the IDW method is the optimal technique to generate a digital surface with less uncertainty.

The study highlights the importance of selecting appropriate interpolation methods for bathymetric modeling. It demonstrates the superiority of IDW for generating accurate and high-quality digital bathymetric surfaces for shallow water coasts. Notably, our research has identified the optimal interpolation method that can be given preference over other methods when the extent of the study area is circular and well-distributed points exist.

Acknowledgments. The authors gratefully acknowledge the science teams of ICESat-2 for providing access to the data. This work was conducted with the infrastructure provided by the National Remote Sensing Centre (NRSC), for which the authors were indebted to the Director, NRSC, Hyderabad. We acknowledge the continued support and scientific insights from Dr. S. K. Srivastav and Dr. Apurba Kumar Bera, Mr. Rakesh Fararoda, Mr. Sagar, S. Salunkhe, Mr. Hansraj Meena, and other staff members of Regional Remote Sensing Centre – West, NRSC/ISRO, Jodhpur. This research did not receive any specific grant from funding agencies in the public, commercial, or not-for-profit sectors.

References

Amoroso, P. P., U. Falchi, F. G. Figliomeni, and A. Vallario (2023), The Influence of Interpolation Methods and point density on the Accuracy of a Bathymetric Model, in *2023 IEEE International Workshop on Metrology for the Sea; Learning to Measure Sea Health Parameters (MetroSea)*, pp. 148–153, IEEE, https://doi.org/10.1109/MetroSea58055.2023.10317127.

Ashphaq, M., P. K. Srivastava, and D. Mitra (2021), Review of near-shore satellite derived bathymetry: Classification and account of five decades of coastal bathymetry research, *Journal of Ocean Engineering and Science*, *6*(4), 340–359, https://doi.org/10.1016/j.joes.2021.02.006.

Becker, M., M. Karpytchev, and F. Papa (2019), Hotspots of Relative Sea Level Rise in the Tropics, in *Tropical Extremes*, pp. 203–262, Elsevier, https://doi.org/10.1016/B978-0-12-809248-4.00007-8.

Brown, M. E., S. D. Arias, and M. Chesnes (2023), Review of ICESat and ICESat-2 literature to enhance applications discovery, *Remote Sensing Applications: Society and Environment*, *29*, 100,874, https://doi.org/10.1016/j.rsase.2022.100874.

Burrough, P. A., R. A. McDonnell, and C. D. Lloyd (2015), *Principles of geographical information systems*, 432 pp., Oxford University Press, USA.

Childs, C. (2004), *Interpolating surfaces in ArcGIS spatial analyst*, ArcUser.

Collet, S., T. Kidokoro, P. Karamchandani, and T. Shah (2018), Future-Year Ozone Isopleths for South Coast, San Joaquin Valley, and Maryland, *Atmosphere*, *9*(9), 354, https://doi.org/10.3390/atmos9090354.

de Souza, E. C. B., C. P. Kruger, and C. R. Sluter (2003), Determinação das variações volumétricas no ISTMO da ilha do mel utilizando PDGPS, *Boletim de Ciências Geodésicas*, *9*(1), 53–74.

Devi, P. Y., and X. Xi (2020), The impacts of climate change on the coastal zone of Mauritius, *Journal of East China Normal University (Natural Science)*, *2020(S1)*(104), https://doi.org/10.3969/j.issn.1000-5641.202092213.

Doorga, J. R. S., M. Sadien, N. A. Bheeroo, et al. (2021), Assessment and management of coastal erosion: Insights from two tropical sandy shores in Mauritius Island, *Ocean & Coastal Management*, *212*, 105,823, https://doi.org/10.1016/j.ocecoaman.2021.105823.

Duvat, V. K. E., A. Anisimov, and A. K. Magnan (2020), Assessment of coastal risk reduction and adaptation-labelled responses in Mauritius Island (Indian Ocean), *Regional Environmental Change*, *20*(4), https://doi.org/10.1007/s10113-020-01699-2.

Dysart, P. S. (1996), Bathymetric surface modeling: A machine learning approach, *Journal of Geophysical Research: Solid Earth*, *101*(B4), 8093–8105, https://doi.org/10.1029/95JB03737.

ESRI (2024a), GIS Software for Mapping and Spatial Analytics, https://www.esri.com.

ESRI (2024b), How Kriging works, https://pro.arcgis.com/en/pro-app/tool-reference/3d-analyst/how-kriging-works.htm.

Ferreira, I. O., D. D. Rodrigues, G. Rodrigues dos Santos, and L. M. F. Rosa (2017), In bathymetric surfaces: IDW or Kriging?, *Boletim de Ciências Geodésicas*, *23*(3), 493–508, https://doi.org/10.1590/S1982-21702017000300033.

GAGE Facility (2021), Geoid Height Calculator, https://www.unavco.org/software/geodetic-utilities/geoid-height-calculator/geoid-height-calculator.html.

Giribabu, D., R. Hari, J. Sharma, et al. (2023), Prerequisite Condition of Diffuse Attenuation Coefficient Kd(490) for Detecting Seafloor from ICESat-2 Geolocated Photons During Shallow Water Bathymetry, *Hydrology*, *11*(1), 11, https://doi.org/10.11648/j.hyd.20231101.12.

Giribabu, D., R. Hari, J. Sharma, et al. (2024), Performance assessment of GEBCO_2023 gridded bathymetric data in selected shallow waters of Indian ocean using the seafloor from ICESat-2 photons, *Marine Geophysical Research*, *45*(1), https://doi.org/10.1007/s11001-023-09534-z.

Guo, X., X. Jin, and S. Jin (2022), Shallow Water Bathymetry Mapping from ICESat-2 and Sentinel-2 Based on BP Neural Network Model, *Water*, *14*(23), 3862, https://doi.org/10.3390/w14233862.

Hawker, L., and J. Neal (2021), FABDEM V1-0, https://doi.org/10.5523/BRIS.25WFY0F9UKOGE2GS7A5MQPQ2J7.

Henrico, I. (2021), Optimal interpolation method to predict the bathymetry of Saldanha Bay, *Transactions in GIS*, *25*(4), 1991–2009, https://doi.org/10.1111/tgis.12783.

Hilldale, R. C., and D. Raff (2007), Assessing the ability of airborne LiDAR to map river bathymetry, *Earth Surface Processes and Landforms*, *33*(5), 773–783, https://doi.org/10.1002/esp.1575.

INHO (2024), National Hydrographic Office, https://hydrobharat.gov.in.

Li, J., and A. D. Heap (2014), Spatial interpolation methods applied in the environmental sciences: A review, *Environmental Modelling & Software*, *53*, 173–189, https://doi.org/10.1016/j.envsoft.2013.12.008.

Li, Z., Z. Peng, Z. Zhang, et al. (2023), Exploring modern bathymetry: A comprehensive review of data acquisition devices, model accuracy, and interpolation techniques for enhanced underwater mapping, *Frontiers in Marine Science*, *10*, https://doi.org/10.3389/fmars.2023.1178845.

Luo, W., M. C. Taylor, and S. R. Parker (2007), A comparison of spatial interpolation methods to estimate continuous wind speed surfaces using irregularly distributed data from England and Wales, *International Journal of Climatology*, *28*(7), 947–959, https://doi.org/10.1002/joc.1583.

Markus, T., T. Neumann, A. Martino, et al. (2017), The Ice, Cloud, and land Elevation Satellite-2 (ICESat-2): Science requirements, concept, and implementation, *Remote Sensing of Environment*, *190*, 260–273, https://doi.org/10.1016/j.rse.2016.12.029.

Mesić Kiš, I. (2016), Comparison of Ordinary and Universal Kriging interpolation techniques on a depth variable (a case of linear spatial trend), case study of the Šandrovac Field, *Rudarsko-geološko-naftni zbornik*, *31*(2), 41–58, https://doi.org/10.17794/rgn.2016.2.4.

National Snow and Ice Data Center (2023), OpenAltimetry: Visulize and download surface elvevation data from across the Earth, over time, https://openaltimetry.earthdatacloud.nasa.gov/data/.

Neumann, T. A., A. J. Martino, T. Markus, et al. (2019), The Ice, Cloud, and Land Elevation Satellite-2 mission: A global geolocated photon product derived from the Advanced Topographic Laser Altimeter System, *Remote Sensing of Environment*, *233*, 111,325, https://doi.org/10.1016/j.rse.2019.111325.

Parrish, C., L. Magruder, A. Neuenschwander, et al. (2019), Validation of ICESat-2 ATLAS Bathymetry and Analysis of ATLAS's Bathymetric Mapping Performance, *Remote Sensing*, *11*(14), 1634, https://doi.org/10.3390/rs11141634.

Pratomo, D. G., R. A. D. Safira, and O. Stefani (2023), A comparison of different GIS-based interpolation methods for bathymetric data: case study of Bawean Island, East Java, *Geodesy and cartography*, *49*(4), 186–194, https://doi.org/10.3846/gac.2023.18250.

Ranndal, H., P. Sigaard Christiansen, P. Kliving, O. Baltazar Andersen, and K. Nielsen (2021), Evaluation of a Statistical Approach for Extracting Shallow Water Bathymetry Signals from ICESat-2 ATL03 Photon Data, *Remote Sensing*, *13*(17), 3548, https://doi.org/10.3390/rs13173548.

Sibson, R. (1981), A Brief Description of Natural Neighbor Interpolation, in *Interpolating Multivariate Data*, John Wiley & Sons, New York.

Smith, W. H. F., and D. T. Sandwell (1997), Global Sea Floor Topography from Satellite Altimetry and Ship Depth Soundings, *Science*, *277*(5334), 1956–1962, https://doi.org/10.1126/science.277.5334.1956.

Vogt, P. R., and B. E. Tucholke (1986), Imaging the ocean floor: History and state of the art, pp. 19–44, https://doi.org/10.1130/DNAG-GNA-M.19.

Wang, S., G. H. Huang, Q. G. Lin, et al. (2014), Comparison of interpolation methods for estimating spatial distribution of precipitation in Ontario, Canada, *International Journal of Climatology*, *34*(14), 3745–3751, https://doi.org/10.1002/joc.3941.

Watson, D. (1992), *Contouring: A Guide to the Analysis and Display of Spatial Data*, Pergamon Press, London.

Wölfl, A.-C., H. Snaith, S. Amirebrahimi, et al. (2019), Seafloor Mapping - The Challenge of a Truly Global Ocean Bathymetry, *Frontiers in Marine Science*, *6*, https://doi.org/10.3389/fmars.2019.00283.

Xie, C., P. Chen, D. Pan, C. Zhong, and Z. Zhang (2021), Improved Filtering of ICESat-2 Lidar Data for Nearshore Bathymetry Estimation Using Sentinel-2 Imagery, *Remote Sensing*, *13*(21), 4303, https://doi.org/10.3390/rs13214303.